EFDA–JET–PR(08)10

L.-G. Eriksson, T. Hellsten, M.F.F. Nave, J. Brzozowski, K. Holmström,
T. Johnson, J. Ongena, K.-D. Zastrow and JET EFDA contributors

Toroidal Rotation in RF Heated JET Plasmas

Toroidal Rotation in RF Heated JET Plasmas

L.-G. Eriksson[1], T. Hellsten[2], M.F.F. Nave[3], J. Brzozowski[2], K. Holmström[2], T. Johnson[2], J. Ongena[4], K.-D. Zastrow[5] and JET EFDA contributors*

JET-EFDA, Culham Science Centre, OX14 3DB, Abingdon, UK

[1]*Association EURATOM-CEA, CEA/DSM/DRFC, CEA-Cadarache, F-13108 St. Paul lez Durance, France*
[2]*Association EURATOM-VR, Department of Physics, SCI, KTH, SE-10691 Stockholm, Sweden*
[3]*Associação EURATOM/IST, Instituto de Plasmas e Fusão Nuclear, Instituto Superior Técnico, Av Rovisco Pais, 1049-001 Lisbon, Portugal*
[4]*Association "EURATOM - Belgian State" Laboratory for Plasma Physics Koninklijke Militaire School Ecole Royale Militaire Renaissancelaan 30 Avenue de la Renaissance B-1000 Brussels Belgium,*
[5]*EURATOM-UKAEA Fusion Association, Culham Science Centre, OX14 3DB, Abingdon, OXON, UK*
** See annex of M.L. Watkins et al, "Overview of JET Results ", (Proc. 21st IAEA Fusion Energy Conference, Chengdu, China (2006)).*

Preprint of Paper to be submitted for publication in
Plasma Physics and Controlled Fusion

ABSTRACT.
Observations of bulk plasma rotation in Radio Frequency (RF) heated JET discharges are reported. The study is concentrated on RF heated L mode plasmas. In particular, the toroidal rotation profiles in plasmas heated by Ion Cyclotron Resonance Frequency (ICRF) waves and Lower Hybrid (LH) waves have been analysed. It is the first time that rotation profiles in JET plasmas with LH waves have been measured in dedicated discharges. It is found that the toroidal plasmas rotation in the outer region of the plasmas is in the co-current direction irrespective of the heating scenario. An interesting feature is that the toroidal rotation profile appears to be hollow in many discharges at low plasma current, but a low current in itself does seem not to be a sufficient condition for finding such profiles. A loss of fast ions is one mechanism that could explain hollow rotation profiles. This possibility has been investigated by numerical simulations of the torque on the bulk plasma due to fast ICRF accelerated ions. The obtained torque is used in a transport equation for the toroidal momentum density to estimate the effect on the thermal bulk plasma rotation profile.

1. INTRODUCTION

Plasma rotation can play an important role in fusion plasmas. In particular, strong shear in the rotation, or more precisely in the toroidal velocity component associated with the radial electric field, is widely believed to be an important factor for transport barriers [1, 2]. Another major area where plasma rotation can play a crucial role is resistive wall modes (RWMs), where it has a stabilising influence [3]. In fact, recent experimental results indicate that rather modest plasma rotation can be sufficient to have a beneficial effect [4, 5]. In today's tokamaks the greatest source of torque on the plasmas is due to Neutral Beam Injection (NBI). On the other hand, in ITER or reactor plasmas the torque from NBI should be a less important factor than in present day tokamaks. There are several reasons for this; one is that the injected momentum scales as $P_{NBI}/E_{inj}^{1/2}$ and that the injection energy must be much higher in a dense reactor plasma than in today's machines. Consequently, it is of interest to study other mechanisms that can give rise to plasma rotation. Intriguing observations of plasmas rotation have been made in RF heated plasmas with little or no external momentum injection [6-16]; this phenomenon is often referred to as "intrinsic" rotation. Toroidal rotation in both the direction of the plasma current and in the opposite direction has been observed. Most observations in H-mode plasmas have been in the co-current direction, while the trend in L mode plasmas is less clear. It is possible that there are different dominating mechanisms behind the observed rotation in L and H mode plasmas. While the toroidal rotation found in plasmas with low external momentum input usually is modest compared to plasmas heated by NBI in today's tokamaks, an important question is if it is significant enough to provide a useful contribution to resistive wall mode stabilisation in ITER and reactor plasmas. Unfortunately, the origin of the observed rotation is not well understood, and it is at present difficult to make theoretical predictions. Work has therefore been initiated on establishing a multi-machine database in order to study the scaling of the rotation with different dimensionless parameters [17]. The present state of this scaling indicates that the extrapolated intrinsic toroidal rotation in ITER might be sufficient to stabilize resistive wall modes. It is therefore important to develop a better understanding of the mechanisms behind the intrinsic rotation so that one could be more confident in predictions for ITER and other future machines. In order to achieve this, both efforts in theory development and further experiments are needed. While it is important to understand rotation in H-mode plasmas, which is the main focus in Ref. [17], it is also of interest to gain a better understanding of its origin in L mode plasmas. Not least because a discharge has to go through an L-mode phase before a transition into H-mode is made. The experimental results on toroidal plasmas rotation presented in this paper were obtained in JET L-mode plasmas, and allow for a more extensive statistical analysis than has earlier been presented for such JET discharges.

The theoretical effort aimed at understanding the origin of intrinsic rotation has resulted in several theories being put forward. Since many of the initial observations of rotation in low momentum input plasmas were reported in ICRF heated plasmas, theories relating to fast ICRF accelerated ions have been proposed. While counter current rotation in some cases could be due to loss of fast trapped ions (an ion is travelling in the co-current direction on the outer leg of its orbit, and a loss of it will therefore give a counter current torque on the plasma), there is no equally obvious mechanism for co-current rotation. However, as pointed out in Ref. [18], no net torque on the plasma is needed to give rise to plasma rotation. It is sufficient to have dipolar torque (whose integral over the plasma is zero) and radial transport of the toroidal momentum. Owing to finite orbit width effects and spatial transport of the resonating ions, there is always such a dipolar torque present in ICRF heated plasmas. The theory predicts co/counter current rotation if the inner lobe of the dipolar torque is in the co/counter current direction. The analysis in Ref. [18] and subsequent investigations of the theory, see e.g. [19, 20], indicated that in order to have an inner lobe of the dipolar torque in the co/counter current direction, the ICRF resonance layer should be on the low/high field side of the magnetic axis. Thus, this particular theory would tend to predict co-current rotation for low field side resonances and counter-current rotation for high field side ones. This change in the rotation direction has not been supported by experimental observations see e.g. [11, 8]. Thus, while the effect clearly should be present, it does not appear to be the dominating one. Another possibility that was briefly mentioned in Ref. [20] is that even when the launched antenna spectrum is symmetric, the amount of power absorbed by the resonating ions need not be equal for positive and negative toroidal mode numbers. This is due to the fact that the Doppler shift separates the points where resonant wave particle interaction takes place for co and counter current propagating waves. Finite orbit width effects also play a role in the process. Since the waves carry momentum, the resulting imbalance will lead to a torque on the plasma, which is first absorbed by the fast ions and then transferred to the bulk plasma. The experimental evidence presented in Ref.[21], where the phasing of the JET ICRF antennas was varied from launching waves propagating predominantly in the direction of the plasma current to counter-current propagating ones, is relevant for this hypothesis. By changing the antenna phasing in this way, one ensures that the imbalance between power absorbed from waves with positive and negative toroidal mode numbers is strong. It was indeed possible to detect a difference in the rotation when the phasing of the antennas was changed, which was consistent with the difference in absorbed wave momentum. However, in all cases, i.e. irrespective of the phasing, the plasma was found to rotate in the co-current direction. Thus, there appeared to be an underlying effect, not directly related to the absorption of ICRF power, which dominated the observed rotation.

In view of the difficulties of explaining the observed rotation by effects purely related to the heating mechanism and fast ions, it looks likely that a bulk plasma effect is involved. This conjecture was reinforced by the results on Alcator C-mod, which indicated that plasmas in Ohmic H-modes also rotated in the co-current direction with a similar scaling to ICRF heated plasmas. Consequently, theoretical effort has been devoted to study bulk transport effects and their relation to toroidal rotation. Early neo-classical theory [22], predicted rather strong counter current rotation in Ohmic plasmas, but in view of the fact that the momentum transport in the core plasma is most likely anomalous, this prediction is probably less relevant. In order to explain the observed rotation in Alcator C-Mod, which normally operates at high density, a neo-classical theory was developed for the edge region in the Pfirsch-Schl¸ter regime [23], for those conditions co-current rotation was predicted in Alcator C-Mod consistent with the observations [10]. However, many other tokamaks like JET are rather in the banana regime, and the co-current rotation observed in such conditions, e.g. reported in the present paper, cannot be directly explained by the theory of [23]. Neo-classical effects associated with magnetic field ripple can also influence plasma rotation [24]. First there is breaking force due to the friction between ripple well trapped ions and the rest of the plasma. There is also a thermal type of force due to collisions between poloidally trapped ions and ripple well trapped ones [25], it arises due to the finite orbit width of the polidally trapped ions. If not dominated by other effects, the balance between the ripple induced thermal force and breaking would lead to a co-current rotation proportional to the ion temperature gradient [25]. Moreover, there are torques associated with ripple induced transport of non-thermal ions. However, under normal operation in JET, the ripple is too small for these effects to play a significant role. Turbulent transport offers other mechanisms that can drive rotation. For example, flows driven in the scrape of layer by what appears to be ballooning type transport was reported from Alcator C-mod in Ref. [26], theoretical considerations indicate that there should be a concomitant finite volume averaged co-current momentum if the ion grad-B drift direction is towards the divertor and counter-current if the drift is away from it. Another theory relying turbulent transport is the so called accretion theory put forward in Ref. [27], where the preferential direction of the turbulent modes in the edge of the plasma is invoked to provide a torque on the plasma. The theory suggests that plasmas in H-mode should rotate in the co-current direction, consistent with e.g. observations on JET and Alcator C-Mod [7, 9-12]. However, co-current rotation is observed also in JET L-mode plasmas [8], which is not readily explained by the basic factors discussed in [27]. A recent theory based on transport driven by drift wave turbulence reported in Ref. [28] suggests that symmetry breaking due to $\vec{E} \times \vec{B}$ shearing in H-mode plasmas leads to a pinch term in the transport equation for the toroidal momentum density. The implication is that this could explain the co-current acceleration often observed at the transition into H-mode (see [7, 9-12]). A turbulent momentum pinch based on symmetry breaking due to magnetic field curvature is discussed in Ref. [29]. It relies on toroidal effects and should be present also in L mode plasmas. Another pinch term, due to Coriolis drift effects, has recently been discussed in Ref. [30]. Moreover, off-diagonal terms in the transport matrix are likely to play a role [31]. However, no systematic quantitative comparisons with experimental results have yet been provided for these pinch and off-diagonal terms, and it is therefore not yet clear how important they are in reality.

The brief review above of mechanisms that could be involved in the generation of toroidal rotation in plasmas with little external momentum input indicates the complexity of the problem. While many of the theories put forward might not provide a dominating mechanism, there is no doubt that several of them may be contributing for any given discharge. Thus, in order to try to assess the importance of individual effects, a large data base of experimental discharges is required. In particular, it is essential that it includes reliable measurements of the toroidal rotation profiles. Such measurements can provide valuable information on various effects, and could hint to the regions where they are effective. In an effort to contribute to such a data base, a number of discharges aimed at measuring toroidal rotation profiles were carried out during 2006 and 2007 in JET. These were mainly concentrated on studying discharges in L-mode because rotation in such plasmas is generally less well documented. An important factor that was investigated in the series of discharges presented here was the safety factor, q-, profile. In order to create a q-profile with q above unity everywhere (and also slightly hollow), Lower Hybrid Current Drive (LHCD) was applied. These discharges were the first in JET dedicated to measuring rotation profiles in plasmas with LHCD. The aim of the present paper is to describe the main features of the data base of discharges acquired during 2006 and 2007. The scaling with different parameters of the rotation of the central part of the plasma has been studied as well as that of the outer region.

In order to assess the influence of fast ICRF accelerated fast ions on the rotation profiles discussed in this paper, simulations of the torque they exert on the bulk plasma have been carried out. A comprehensive modelling of the ICRF power deposition and its influence on the distribution function of the resonating ions was used for this purpose. The simulated torques were then inserted in to a simple momentum diffusion equation to estimate the influence on the rotation profiles.

2. MEASUREMENT TECHNIQUE

The main diagnostic used for measuring the rotation profiles was Charge Exchange Recombination Spectroscopy (CXRS). Because this method requires diagnostic NBI, the rotation profile is perturbed by the momentum carried by the injected particles. In order to minimize this, only short beam pulses and low power, typically 200 ms at 1-3 MW, has been used. Moreover, only the first CXSR spectrum after the application of each NBI pulse was used to deduce the rotation velocity. This method was extensively discussed Ref [8], where it was shown that the perturbation caused by the

NBI pulses was acceptably small. Furthermore, it should be noted that results discussed in Ref. [8] were obtained with an integration time of 50ms; the JET CXRS has been upgraded since then [32], allowing for an integration time of only 10ms. The rotation profiles shown in this paper were obtained with this shorter integration time, and the perturbations should therefore be even smaller than suggested in Ref [8]. Typical power wave forms for the discharges discussed in this paper is shown in Fig.1. All the discharges had similar power wave forms. However, the timing of the ICRF heating was varied, power was applied both early and late in the discharge to study the influence of the q-profile. The evolution of the central toroidal rotation velocity measured by CXRS during an NBI pulse is also shown in Fig. 1. It is in the centre that the perturbation due to the diagnostic beam is greatest; towards the edge the influence is very small. From figure 1 one can see that the perturbation is typically of the order 1-2 krad/s in the injection (i.e. co-current) direction. This "error bar" should be kept in mind when assessing the rotation profiles.

The weakness of the CXRS measurement, apart from the perturbation caused by the diagnostic beam, is that only snapshots of the rotation profiles are obtained. Unfortunately, the x-ray crystal spectrometer [33] at JET was only working partially for the discharges discussed in this paper; it would otherwise have routinely produced the time evolution of the toroidal rotation near the centre. In order to have additional information on the temporal evolution of the toroidal rotation, MHD activity has been analysed. From the observed frequency of MHD modes, the toroidal rotation of the plasma at the mode location can be deduced non-perturbatively. The frequency of sawtooth precursors has mainly been used for the present study.

3. EXPERIMENTAL RESULTS

The discharges presented here were carried out mainly in L-mode plasmas, with an ICRF power up to 7MW. The magnetic field was between 2.4 and 2.8T, with the majority of the discharges being run with 2.6T. It should be noted that at this field, the available ICRF power was not sufficient to take the discharges into H-mode. The plasma current was varied between 1.2MA and 2.6MA. The ICRF heating scenario was hydrogen minority heating in deuterium plasmas, (H)D. Three different ICRF frequencies were used: 37, 42 and 48 MHz, which together with the variation of the magnetic field caused the hydrogen cyclotron resonance layer to be located between 0.5m on the high field side and 0.45m on the low field side. In most of the discharges dipole phasing of the JET antennas was used, which produces a symmetric toroidal mode number spectrum of the launched waves. This should ensure that the external momentum input from the waves is small, but not necessarily zero as discussed in the introduction. In order to test the influence of the q-profile on the toroidal plasma rotation, a few discharges also had LH power of up to 2MW applied in the current ramp-up phase. In this way discharges with low or slightly reversed central shear were created.

Let us first consider JET discharge #66302, for which the tororidal rotation deduced from MHD activity is available as well as the rotation profile from CXRS. The magnetic field and current in the discharge was 2.6T and 2.5MA respectively, the ICRF resonance layer for the hydrogen minority ions was located about 40 cm on the high field side of the magnetic axis. The power wave form for this discharge as well as the spectrogram from the magnetic pick-up coils is shown in Fig. 2. The activity visible on the spectrogram is due to sawtooth precursors. It can clearly be seen that the mode frequency increases when the ICRF power is applied. Moreover, the effect of the NBI pulses is clearly visible. While an increase in the diamagnetic drift frequency, ω_{*i}, could contribute to the change in mode frequency, the evolution of the ion temperature in response to the applied ICRF power is not strong enough to explain observed change of the mode frequency (the ICRF accelerated hydrogen ions tend to become very energetic, and consequently the absorbed power transferred via them to the bulk plasma through collisions mainly goes to the electrons). Furthermore, there is no evidence that the location of the modes changed. Thus, the change in the mode frequency should be mainly due to an acceleration of the plasma. An increase of the mode frequency corresponds to a co-current acceleration. This is confirmed by the increase in the mode frequency at the application of the NBI pulses, which provided a net momentum in the co-current direction. The evidence from the spectrogram shows that the plasma accelerated in the co-current direction at the application of the ICRF power, resulting in a change of the toroidal rotation frequency by about 6-7 krad/s. This can be compared to the CXSR measurements, Fig.3, which show a rotation velocity in the centre of the discharge of about 8krad/s at the beginning of the third NBI pulse at t=63.015sec. The rotation profile is slightly peaked and the plasma is rotating in the co-current direction. Unfortunately, the rotation profile in the Ohmic phase was not measured in this discharge. However, the CXRS measured central co-current rotation of 8krad/s together with the observed 6-7krad/s acceleration of the plasma in the co-current direction suggest that the rotation velocity was low in the Ohmic phase before the application of the ICRF power.

Another useful piece of information that can be obtained from the time evolution of the rotation frequency in the central region of Pulse No: 66302 is the confinement time of the momentum. After the application of the NBI pulses the rotation velocity can be seen to decay on a time scale of 0.3 seconds, and the confinement time of the toroidal momentum, τ_M, should be of the same order. Since the energy confinement time in the plasma was around 0.4 seconds we find, $\tau_M \sim \tau_E$ in this discharge. This is consistent with a wide variety of findings in different devices that indicates that the momentum and energy confinement times normally are of the same order, see e.g. [34, 43]. In view of this, $\tau_M \sim \tau_E$ has been assumed in the simulations presented in section 4. However, as discussed in section 4, this does not automatically mean that one can assume that the energy and momentum diffusivities are close to being equal.

Let us now have a more detailed look at the measured rotations profiles in a few discharges. One of the most striking features of the discharges reported in this paper was that hollow rotations profiles were observed in many of them at low current, typically 1.5MA, whereas the rotation profiles at higher currents, typically 2.3MA and higher, were mostly relatively flat or weakly peaked. This is illustrated in Figure 4, which shows one discharge with I_p= 1.5MA (Pulse No: 66310) and a second with I_P = 2.5MA (Pulse No: 66315). Both had a magnetic field of 2.6T and dipole phasing of the antennas was used with a frequency was 47MHz, placing the hydrogen minority cyclotron resonance about 40cm on the high field side of the magnetic axis. It is interesting to note that the rotation frequency in the edge region is in the co-current direction and almost the same in the two discharges. In fact, the edge region was found to rotate in the co-current direction for all the discharges discussed in this paper. What is shown in Fig.4 is the total toroidal rotation velocity and it is of course of interest to determine the difference between the Ohmic phase and the one when the ICRF power was applied. In some discharges, but not all, there was an NBI pulse to measure the rotation profile also in the Ohmic, post ICRF phase (in fact an NBI pulse in the Ohmic phase was programmed for almost all the discharges, but for technical reasons the NBI could not always fire in that phase). There is of course no guarantee that the rotation in the post ICRF phase is similar to that before the ICRF is applied. Thus, it should be kept in mind that taking the difference between the rotation profiles in the ICRF phase and the Ohmic post ICRF phase does not necessarily represent a general difference between Ohmic plasmas and ICRF heated ones. In Pulse No: 66310 the rotation profile in the Ohmic phase was measured, and the differences in rotation profiles between those taken at the beginning of the first three NBI pulses and the last one are shown in Fig. 5. The profile taken at the first NBI pulse shows a difference in the co-current direction, while the subsequent two rotation profiles show that the central plasma rotation was thereafter changing in the counter current direction, leading to the hollow profile shown in Fig. 4. It should, however, be noted that the rotation profile in the Ohmic phase also was slightly hollow. In order to make sure this was not a lingering effect of the rotation having been hollow in the ICRF phase, a discharge without ICRF, but with the same diagnostic NBI pulses and current as in Pulse No: 66310, was carried out. The rotation profiles taken at the last two NBI pulses in this Pulse No: 6399, are shown in Fig.6 (in fact the rotation profiles from the four NBI pulses were similar). As can be seen, the rotation profiles are hollow. Furthermore, since the central part of the plasma is accelerated in the co-current direction during the application of the NBI (similar to what is shown in Fig.1), the rotation profile is returned to hollow between the NBI pulses. It therefore appears that hollow rotation profiles might occur naturally in JET plasmas with low current. The rotation frequency in the centre of Pulse No: 66399 is stronger in the counter current direction than in the post ICRF phase of Pulse No: 66310, which illustrates the uncertainty associated with determining an Ohmic level for the type of difference taken in Fig.5. In discharges with higher current, I_p > 2.3MA, the rotation profiles in the Ohmic post ICRF phase, where rotation measurements were possible, have not shown the same tendency for hollowness as at low current. To return to effect of the ICRF, in spite of the fact that the rotation profiles can be hollow already in the Ohmic phase, the evidence of Fig.5 indicates that at the later stage of the discharge the addition of ICRF power makes the rotation profile more hollow, with the central part rotating in the counter current direction. This could be a sign of the influence of fast ICRF accelerated ions; a question addressed in some detail in section 4, where simulations of the influence of the fast ions on the rotation are discussed. The effect of the fast ions on the rotation should also depend on whether the minority cyclotron resonance is on the low or high field side. A few discharges were therefore carried out with the hydrogen minority cyclotron resonance about 40 cm on the low field side of the magnetic axis). In the discharge of these with the highest ICRF power level, the rotation profile stayed flat despite the fact that a low current of 1.5MA was used. However, there are too few discharges of this type in the database discussed here to draw any firm conclusions on the difference in rotation between high and low field side resonances.

The slightly peaked rotation profile found in the high current discharge of Fig.4 is typical of what was found in such discharges. Unfortunately, there was no NBI pulse in the Ohmic phase of this discharge, so the difference between the ICRF and Ohmic phases cannot be obtained. In order to find a good high current discharge that has a measured rotation profile in the Ohmic post ICRF phase we can consider Pulse No: 66394, although it had a slightly lower field and current: 2.4T and 2.4MA. The toroidal rotation profiles for this discharge are shown in Fig.7, again the difference in rotation profiles between those in the ICRF phase and that in the Ohmic post ICRF phase are shown. A clear co-current acceleration in the centre can be seen in Fig.7 when the ICRF power is applied. It should be noted that the rotation profile in the Ohmic phase of the discharge was fairly flat with a rotation frequency of around 2krad/s in the outer region of the plasma. While it is possible to imagine that the fast ions could have a significant influence at lower plasma currents, they ought to play a lesser role at high currents. In particular, it is difficult to see how they could contribute to co-current toroidal rotation in the centre (c.f. [18, 20]). In order to try to confirm this view, experiments with different minority concentrations were carried out. Since the averaged energy of the resonating ions depends strongly on the concentration of minority ions (roughly inversely proportional), one would think that their potential influence on the rotation should be quite different at high and low minority concentrations. A comparison of two discharges at high current, $I_p = 2.5$MA, is shown in Fig.8. One had a concentration of about $n_H/n_D \approx 2.5$ % and the other with $n_H/n_D \approx 12$ %, in other respects they were similar. There appears to be some differences between the rotation profiles, with the discharge at a higher concentration showing a somewhat more peaked profile. However, the differences are quite small, suggesting that the fast ions are not involved in the dominating process giving rise to the rotation.

In order to get an overview of the trends in the L mode discharges discussed here, a database comprising 20 shots has been established. The discharges had ICRF heating with dipole phasing of the antennas, and the rotation profiles taken from the first CRXS spectra at all the NBI pulses are included in this database. Since the number of discharges which have rotation profiles measured in the Ohmic phase is limited, only the total rotation frequency is considered here. Different scalings for the edge and core rotation frequencies have been tested against the rotation data; here the rotation velocity at the edge has been taken from the measurement point closest to 3.7m (corresponding roughly to $r/a \approx 0.8$), while the central rotation has been characterised by the measured velocity at the point closest to 3.1m. A large number of combinations of various plasma parameters have been tried. The best scaling for the edge rotation was found when it was plotted against the diamagnetic stored energy, W_{DIA}, divided by the line integrated electron density. The resulting scaling is shown in Fig.9. This is different from the W_{DIA}/I_p scaling reported for ICRF heated (and Ohmic) H-modes from Alctor C-Mod [9-11]. One obvious difference is that the discharges in the database reported here were in L-mode. This could suggest that there are different dominating mechanisms that give rise to the observed rotation in L and H mode plasmas. On the other hand, it is also interesting to note that the rotation in the edge region scales with bulk plasma quantities rather than others, like the ICRF power, directly linked to the heating process. It is therefore likely that the dominating mechanism originates from the bulk plasma physics. However, as the example in [18] shows, one can find scalings that depend on bulk plasma parameters even for a mechanism relying on fast ions. Thus, some caution is called for. Nevertheless, the fact that the rotation in the edge region, where there are few fast ions, scales with the diamagnetic stored energy indicates that it most likely is related to a process in the bulk plasma.

It is more challenging to find a good scaling for the rotation in the centre. To date, the best one found simply relates the toroidal rotation frequency in the centre to the plasma current, see Fig. 10. In accordance with the discussion of single discharges above, hollow profiles, with in several cases counter current rotation in the centre, are found in many of the discharges with plasma currents below 2.3MA. However, in line with the findings for the rotation profile at the first NBI pulse in Fig.5, it is not necessarily the case that the rotation profile is hollow at low current. On the other hand, all of the discharges at high current, I_p > 2.3MA, had fairly flat or somewhat peaked rotation profiles.

It would obviously be of interest to try to understand why hollow rotation profiles are found at low currents, but not at higher ones. As already mentioned, fast particle effects could have an influence on the central rotation, but there are also a number of other possible effects. For instance, there is sawtooth activity in most of the discharges, and it is possible that sawteeth could influence the plasma rotation, e.g. through the redistribution of the bulk plasma. There could also be a fast ion effect linked to sawtooth redistribution since trapped and passing fast ions are not expected to be redistributed to the same extent. In particular, trapped ions are probably less redistributed than the passing ones [36], while one could expect electrons to be redistributed in a way similar to the passing ions (since both follow field lines). If this is the case a radial electric field arises to ensure quasi-neutrality and at least a temporary acceleration of the central part of the plasma could be envisaged. For this reason and others it is of interest to investigate the possible influence of sawteeth on the rotation. One way of doing this is to change the q-profile, especially to run discharges with q above one everywhere in the plasma. This can be achieved by adding LHCD power to the plasma during the current ramp up phase. Thus, dedicated discharges aimed at studying plasma rotation with slightly reversed q profiles and $q > 1$ where carried out with LHCD applied in the current rise phase. In the process the first rotation profiles in discharges with LHCD and short diagnostic NBI pulses were obtained. The timing and the power wave forms in these discharges had to be modified somewhat. In particular, LHCD was applied early in the discharge to ensure a slow current penetration. Moreover, the discharges had to be fairly short since MHD instabilities caused problems when the q=1 surface appeared in the plasma. It should be noted that the application of LH power can in itself affect the rotation, especially since the LH waves carry wave momentum. This effect is assessed in the next section and is found to be moderate, less than 1krad/s in the centre. The power wave form and the rotation frequency near the centre of the plasma are shown for one such discharge in Fig.11. The central rotation frequency in this discharge was slightly counter current in the centre. The rotation profiles for this discharge and a second one without ICRF power, i.e. only LHCD and NBI pulses, are shown in shown in Fig.12. The profiles are taken from the first NBI pulse at around 4.3 seconds, at this point the plasma current was about 2MA. There is a significant difference between the rotation profiles; the discharge with ICRF power had a hollow profile while the one with LHCD only was slightly peaked. It is also interesting to see in Fig.11 that the plasma centre spins up during the application of the NBI pulse and that the rotation profile has returned hollow at the second NBI pulse. Thus, there appear to be an effect associated with the application of ICRF power that drives the rotation negative in the centre. Breaking due to MHD modes partly locking to the wall could contribute, but it could not change the sign of the rotation. In view of the fact that both the discharges with and without ICRF power were free from sawteeth indicates that effects associated with the sawtooth redistribution are not major factors for the hollowness of the rotation profiles. This is also supported by an analysis of database of discharges, where no direct correlation between quantities associated with the sawteeth and the rotation profiles could be found.

From the experimental results no clear explanation to why many of the low current discharges had hollow rotation profiles has yet been found. The possibility that fast ion effects are involved is investigated in the next section. It seems rather clear, however, that the co-current rotation observed in the outer region of the discharges discussed in this paper has its origin in bulk plasma related physics. It is significant that the co-current rotation is observed even at the outermost measurement point at almost 3.8m, suggesting that an important mechanism for the rotation is related to the physics of the edge plasma.

4. SIMULATIONS OF THE INFLUENCE OF ICRF ACCELERATED FAST IONS AND LH WAVES ON THE TOROIDAL ROTATION

The hollow rotation profiles reported in Figs 5 and 10 could be due to fast ions, especially since they appear at low currents. In the majority of the discharges discussed here the resonance was on the high field side of the magnetic axis. Since ICRF heating tends to drive the turning points of resonating trapped ions towards the cyclotron resonance layer $\omega = \omega_c$, most of them will have their turning points on the high field side for such scenarios. Moreover, the orbits of such trapped particles tend to be wide (for the same energy the orbits are wider if the turnings points are on the high field side as compared to the low field side). In this case there are two effects that could contribute towards a counter current torque in the central region: (i) direct losses of fast ion to the wall, i.e. the most energetic ions could be lost to the wall at low current; (ii) dipolar torque, counter current in centre, due to finite orbit width effects. Losses of fast ICRF accelerated trapped ions give rise to a counter current torque since trapped ions always travel in the co-current direction on the outer leg of their orbits. In the case of a confined orbit with a turning point on the high field side, the inner leg of the orbit can have access to the centre of the plasma. Owing to the fact that trapped ions always travel in the counter-current direction on the inner leg of their orbit, this will give rise to a collisional counter-current torque in the more central part and co-counter one current further out. The situation is, however, more complicated since the radial movement of the fast ions must also be taken into account, which is induced by for instance collisions. The resulting fast ion current is compensated by a radial bulk plasma current and the plasma remains quasi-neutral. The latter current leads to a $\vec{j} \times \vec{B}$ torque on the thermal plasma. It is, however, found that for high field resonances the overall effect is a co-current torque in the centre and a counter current one further out [18-20]. The volume integrated torque is in this case zero, unless, as discussed in the introduction, a torque due to a toroidally asymmetric absorption of waves takes place. Thus, the ICRF accelerated fast ions should have exerted a counter-current torque in the centre in most of the discharges at low current and with high field side resonances.

The brief description above of the mechanisms behind the torque on the bulk plasma due to the resonating ions shows that the process is quite complicated, involving finite orbit width effects and radial transport in real space of the fast ions. Thus, in order to make a realistic assessment of the torque, quite comprehensive modelling is needed. First the propagation and absorption of the ICRF waves must be calculated. Secondly, the effect of the absorbed wave power on the distribution function of the resonating ions has to be simulated. Furthermore, the dielectric properties needed in the wave propagation calculation depend on the distribution function of the resonating ions, necessitating self consistent calculations. In the present paper we use the SELFO code [37] to make the assessment. It is one of the few codes available for such comprehensive simulations. The code combines a full wave code and a 3D Fokker-Planck solver. The latter solves the orbit averaged Fokker-Planck equation with a Monte Carlo method [38], and includes finite orbit width effects and spatial transport of the resonating ions.

In order to assess the effect of the resonating ions on the toroidal rotation of the thermal plasma (i.e. excluding the fast ions) it is not sufficient to calculate the torque. Its effect on the rotation velocity is determined by the transport properties of the toroidal momentum in the thermal plasma. The simplest possible equation for this momentum transport can be written as,

$$n_i m_i \frac{\delta \langle RV_\phi \rangle}{\delta t} = g^{-1/2} \frac{\delta}{\delta \rho} \left[g^{-1/2} n_i m_i \left(\alpha + D \frac{\delta \langle RV_\phi \rangle}{\delta \rho} \right) \right] + t_f + t_o \qquad (1)$$

Where ρ is a flux surface label, V_ϕ is the toroidal velocity (assumed to be the same for all species, which of course is a rough approximation); the Jacobian $g^{1/2}$ is proportional to $dV(\rho)/d\rho$, here V is the volume enclosed by the flux surface; n_i is the density of species i; m_i is the mass of thermal species i (summation over repeated indices is assumed), $\langle \mathbf{L} \rangle$ denotes flux surface average, t_f is the torque density of the fast ions and t_0, is the torque density due to other processes; D is the momentum diffusion coefficient and the term α represents transport of momentum due to off-diagonal terms in the transport matrix and a possible pinch term (proportional to the toroidal velocity), i.e. it can be assumed to have the from

$$\alpha = \alpha_1 V_\varphi + \alpha_2 \frac{f n_i}{f\rho} + \alpha_3 \frac{f T_i}{f\rho} + \dots \tag{2}$$

The details of the momentum transport coefficients are not yet well known. The influence of off-diagonal terms is often thought to be modest [31, 40]. Pinch terms have very recently been discussed in Refs. [28-30], they could be important but they have not yet been extensively evaluated by the wider community. For the simulations presented here we start by neglecting α, and only keep the purely diffusive part. We assume that D increases outwards, similarly to what is normally found for the energy diffusion coefficient. In fact we adopt the model used in Ref. [18], i.e. $D = D_0 [q(\rho)/q_0]^n$, with $n = 2$. As discussed in section 3, experimentally it has been found that the momentum confinement time is close to the energy confinement time for NBI induced torque. We therefore adjust the central value of the momentum diffusion coefficient such that the momentum due to the NBI pulses has a confinement time equal to the energy confinement, which we denote $D_0 = D_{0E}$; for the purpose of calculating D_{0E} we have used torque profiles calculated by the PENCIL code [41]. However, it should be noted that the transport analysis of NBI heated discharges indicate that the Prandtl number (momentum diffusivity over energy diffusivity) normally is less than unity [39, 42] in the core region, typically 0.5 or less. It is been suggested that this could be due to the fact that the profiles of momentum and energy diffusivities are different [42], with the momentum diffusivity being significantly higher in the outer part of the plasma. Thus, NBI momentum deposited in the outer region of the plasma could be lost on a shorter time scale to compensate for the better confinement in the centre, it could therefore be possible to maintain approximately equal energy and momentum confinement times. In the ICRF only cases we discuss here, this might imply that the way we estimate the momentum diffusivity could give too high values. In order to investigate the potential effect of a lower Prandtl number, the simulations have also been run with $D_0 = 0.5D_{0E}$. Furthermore, in order to assess the sensitivity to the radial dependence of the momentum diffusion coefficient, simulations with $n = 0$ have been carried out. There are obviously some differences between the results for n = 2 and $n = 0$, but they are rather minor and the rotation profiles are qualitatively similar in the two cases. For this reason only simulations with $n = 2$ are shown here.

A boundary condition is also needed for the momentum diffusion equation. Since the toroidal rotation velocity is measured almost all the way to the boundary, we simply impose the velocity measured at the outermost CXRS channel (this is similar to many transport simulations, which start from a measured temperature at some point in the outer part of the plasma). This effectively means we assume that the baseline rotation is governed by an effect localised to the plasma boundary. In the absence of a torque from the fast ions and $\alpha = 0$, the rotation profile will then be flat into to the centre. Thus, by adding the torque from the fast ions we can estimate their contribution to the rotation profiles.

Two discharges have been analysedlse Pulse No's: 66307 and 66309. They are similar to those in Fig. 4 (which shows that the measurements were reproducible). Pulse No: 66307 had a plasma current of 2.6MA while Pulse No: 66309 was run with 1.5MA. The power wave forms were the same as in Fig. 1. The measured rotation profiles are shown in Fig.13. The simulated volume integrated torque exerted by the fast ions on the thermal bulk plasma is shown in the top panel of figure 14 for the two discharges, $\alpha = 0$ was used in these simulations. The main difference between the two discharges is that in the low current one fast ions are lost to the wall, which gives rise to a finite total toque (i.e. the volume integrated toque is finite at the boundary). By contrast there are very few fast ion losses in the simulation of the high current discharge. As discussed above, however, despite there being no net total torque, the local torque is not zero. The simulated rotation profiles for the two discharges are shown in the lower panel of Fig. 14. The simulation cannot quite explain the slight peeking of the rotation profile seen experimentally in the high current discharge, especially not for the lower D_0. In the low current discharge there is a clear effect of the fast ions, making the rotation profile hollow. However, it is not nearly as hollow as the measured profile when $D_0 = D_{0E}$. On the other hand, for the reduced value $D_0 = 0.5D_{0E}$, the simulated rotation profile comes fairly close the measured one, i.e. the results could be consistent the lower Prandtl number. However, for the reduced diffusivity, the simulated profile for the high current discharge also becomes quite hollow, which is contrary to the measured rotation profile.

As discussed above, in theoretical work on momentum transport, pinch terms have been reported [28-30] as well as off-diagonal terms, see e.g. [31]. Such terms, represented by α in Eq. (1), are most likely present. One can speculate what they would have to look like to explain the observations. As shown above, the central counter current rotation in the low current discharge could be reproduced if the momentum diffusivity was of the order $D_0 \sim 0.5D_{0E}$ (although some tweaking would be needed to get the whole profile consistent with the observations). In order to reproduce the rotation profile in the high current discharge with $D_0 = 0.5D_{0E}$ one would have to add a term α providing an inward flow of momentum One can of course play with different terms to see their effect on the rotation profile, by adding the pinch term displayed in Fig.15, one can obtain good agreement with the measured profile for Pulse No: 66307 with $D_0 = 0.5D_{0E}$, see Fig.16. On the other hand, when added to the simulation of Pulse No: 6309, the central counter current rotation is no longer reproduced. Thus, it would appear that if pinch or off-diagonal terms play a role for the momentum transport in the two discharges they have to be strongly current dependent. Although of limited value, this experimentation with different terms in the momentum transport equation illustrates the potential complexity of the phenomenon. It should also be mentioned that, like in Pulse No: 66310, Fig.5, there is actually a change in the co-current direction at the first NBI pulse in Pulse No: 66307, and only for the measurements at the two NBI pulses in the higher power phase are hollow profiles found. Thus, it seems very likely several processes are involved. It should, however, be stressed that the influence of the fast ions is important; the simulations clearly show that a significant part of the hollowness in the low current discharges could be explained by fast ion effects. This demonstrates the care that must be taken when making more detailed analyses and scalings of measured data and how difficult it might be to find a single mechanism that explains most of the observed features of the rotation in plasmas with low momentum input

In the discharges where LH power was used to modify the q-profile one should, as has already been mentioned, remember that the waves are directed and therefore carry a finite wave momentum. This momentum is absorbed by the resonant electrons, resulting in a torque on the bulk plasma. Finite orbit width effects are virtually negligible for the fast LH accelerated electrons, but anomalous transport of them would have an effect on the rotation. There is, however, no particular evidence that a significant transport of energetic electrons took place. We therefore concentrate on the absorbed wave momentum and estimate its influence on the rotation. The change in toroidal angular momentum of an electron absorbing an energy ΔW from a wave with toroidal wave number N is given by $\Delta P_\phi = (N/\omega)\Delta W$ (this is a simple consequence of absorption of a wave quantum: $\Delta W = \hbar\omega$ and $\Delta P_\phi = (R\hbar k_\phi = N\hbar)$. Consequently the total torque on the plasma from the LH waves is approximately given by

$$T_{LH} = \frac{Rn_{||}}{c} P_{LH}$$

The parallel refractive index, $n_{||}$, used for the shots in this paper was -1.84 (waves in the counter current direction). With an LH power of 2MW and $R \approx 3$m, we obtain a torque TLH $T_{LH} \cup 0.037$ Nm, which is not negligible. The deposition profile for the LH power is fairly wide, reaching out to around r/a ~ 0.7, and flat for parameters typical of those used in the discharges reported here, see e.g. [44]. Thus, in order to estimate the influence of the LH torque on the plasma, we have assumed a constant deposition profile for the torque density up to r/a = 0.7, with a volume integrated value of 0.037Nm, and have inserted it into the momentum diffusion equation. The momentum diffusion coefficient was obtained in the same way as for the other simulations above (with $\alpha = 0$). This yields a contribution of less than one krad/s in the centre (and less elsewhere). Moreover, it is in the counter current direction and could therefore not be part of the explanation for the central co-current rotation found in the LH only discharge (Pulse No: 68789) shown in Fig.12.

CONCLUSIONS

Rotation in tokamak plasmas with low external momentum is an intriguing phenomenon that is not yet well understood. In view of its potential importance for providing a useful contribution to the plasma rotation needed for stabilising resistive wall modes in ITER and possible future reactor plasmas, it is important to improve the understanding of the underlying effects. Both more extensive databases and theoretical developments are needed. In the present paper we have presented and analysed discharges from a database of JET L-mode discharges with dedicated measurements of toroidal rotation profiles. The database comprises around 20 discharges and present a complement to those discussed in [8]. The discharges were heated by ICRF waves launched by antennas phased such that the total toroidal momentum carried by the waves is small. Furthermore, in order to study the effect of the safety factor profile on the rotation, a few discharges were carried out with added LHCD. In fact, these were the first discharges dedicated to rotation studies with low momentum input in JET in which rotation profiles with LHCD were measured. The measurements relied on charge exchange recombination spectroscopy, using short diagnostic NBI pulses, to obtain rotation profiles. In order to minimise the perturbation of the toroidal rotation from injected momentum, the analysed data were taken only from the first spectra at each NBI pulse. Furthermore, analysis of MHD activity could in some case be used to measure the time evolution of the toroidal velocity at the mode location.

It was found that the rotation in the edge region of the plasma was in the co-current direction for all the discharges in the database. The toroidal rotation frequency scales relatively well with diamagnetic stored energy in the plasma, and the fit of the scaling improved slightly when the stored energy was divided by the line integrated electron density. It is important to note that the rotation in the edge region extended out to the last measurement point of the CXRS, roughly at 3.8m. This suggests that an effect associated with the edge plasma and or scrape off layer is involved. There is no evidence that effects related to fast ions physics are strongly involved in determining the rotation in the outer part of the plasma, instead it is most likely related to the physics of the bulk plasma.

The rotation in the central part of the plasma shows a more complex behaviour. At the higher plasma currents used in the discharges for the present study, the rotation profiles were mostly found to be fairly flat or somewhat peaked. On the other hand, at lower current levels the rotation profiles were often hollow. The rotation velocities were even in the counter current direction in some cases. Interestingly, they were not always hollow at low currents. It has not yet been possible to pin down the exact reason behind this behaviour.

The influence of the q-profile on the rotation was studied by adding LHCD, especially in the current ramp-up phase, to a few discharges. In these the q-profile was slightly reversed and above one when the rotation profiles were measured. An interesting observation was that the rotation profile in a discharge with LHCD only was slightly peaked, while in a similar discharge with added ICRF power, the profile was hollow. This suggests that a process associated with the application of ICRF power contributes to making the rotation profiles hollow. One of the reasons for measuring the rotation profiles in plasmas with $q > 1$ everywhere was to study the influence of sawteeth on the rotation profiles. However, no significant qualitative differences in discharges with ICRF power were found. Furthermore, attempts to correlate the appearance of hollow rotation profiles with e.g. the sawtooth period have not yielded any tangible results.

A contributing factor to the hollow profiles observed at low current could be the torque exerted by the fast ICRF accelerated ions. Simulations of rotation profiles in which the torque obtained with the ICRF code SELFO [37] was inserted in an ad-hoc momentum diffusion equation, indicate that in low current discharges a significant part of the hollowness could be explained by the fast ion torque, but it depends on the details of the momentum transport. In order to reproduce the measured profiles it is not sufficient to use only the torque from the fast ions and a purely diffusive term in the momentum diffusion equation. Instead it would appear that a pinch term or off-diagonal terms in the transport matrix play a role. Moreover, one cannot rule out that other torques could appear (e.g. breaking due to MHD modes partly looked to the wall or low frequency waves excited in by some mechanism in the plasma). These considerations indicate the difficulties involved in establishing multi machine scaling laws for the rotation. For instance, there could be a strong presence of fast ions in one machine and not in another, and to assess mechanisms not related to fast ion torques one has to estimate the influence of the latter. This implies a good knowledge of the momentum transport, which in itself could be an important factor for the rotation in plasmas with low momentum input. Thus, the phenomenon of intrinsic rotation will most likely take time and a significant amount of work to understand in detail,

REFERENCES

[1] T.S. Hahm and K.H. Burrell, Physics of Plasmas **2**, 1648 (1995).
[2] E.J. Synakowski, Plasma Physics and Controlled Fusion **40**, 581 (1998).
[3] A.M. Garofalo, et al., Nuclear Fusion **41**, 1171 (2001).
[4] M. Takechi et al., Physical Review Letters **98**, 055002 (2007).
[5] E.J. Strait et al., Physics of Plasmas 14, 056101 (2007).
[6] L.-G. Eriksson, et al., Plasma Physics and Controlled Fusion **34**, 863 (1992).
[7] L.-G. Eriksson, E. Righi, K.D. Zastrow, Plasma Phys. and Contr. Fusion **39**, 27 (1997).
[8] J.-M. Noterdaeme et al., Nuclear Fusion **43**, 274 (2003).
[9] J.E. Rice, et al., Nuclear Fusion **38**, 75 (1998).
[10] J.E. Rice, et al., Nuclear Fusion **39**, 1175 (1999).
[11] J.E. Rice et al., Nuclear Fusion **41**, 277 (2001).
[12] Lee W.D. et al. Phys. Rev. Lett. **91** 205003 (2003).
[13] Rice, et al., Nuclear Fusion **44**, 379 (2004).
[14] L.-G. Eriksson, G.T. Hoang and V. Bergeaud, Nuclear Fusion **41**, 91 (2001).
[15] J. S. deGrassie et al., Physics of Plasmas **11**, 4323 (2004).
[16] A Scarabosio et al., Plasma Phys. Control. Fusion **48**,†663 (2006)
[17] J.E. Rice at al., Nucl. Fusion **47**, 1618 (2007).
[18] F.W.Perkins, et al., Phys. Plasmas **8**, 2181 (2001).
[19] V. S. Chan, S.C. Chiu, and Y. A. Omelchenko Physics of Plasmas **9**, 501 (2002).
[20] L.-G. Eriksson, F. Porcelli, Nuclear Fusion **47**, 1618 (2002).
[21] L.-G. Eriksson et al., Phys. Rev. Lett. 92 235001 (2004).
[22] Rosenbluth M.N. et al., *Plasma Physics and Nuclear Fusion Research* (IAEA Vienna, 1971) vol. 1, p. 495.
[23] Rogister A. L., et al., *Nucl. Fusion* **42**, 1144 (2002).
[24] A.B. Mikhailovskii, Plasma Physics Reports 21, 529 (1995).

[25] Kuvshinov B. N., Mikhailovskii A. B., et Sharapov S. E., Plasma Physics Reports **21**, 713 (1995).

[26] B. LaBombard et al., et al, Nuclear Fusion 44, 1047 (2004).

[27] B. Coppi, Nuclear Fusion 42, 1 (2002).

[28] Ö. D. G¸rcan, et al., **14**, 042306 (2007).

[29] T.S. Hahm et al., Physics of Plasmas **14**, 072302 (2007).

[30] A.G. Peeters Physical Review Letters **98**, 265003 (2007).

[31] A.G. Peeters et al., Plasma Phys. Control. Fusion **48**, B413 (2006).

[32] C R Negus, et al. , Rev. Sci. Instr. **77**, 10F102 (2006)

[33] F. Bombarda et al, Phys. Rev. A 37 (1988) 504

[34] J.S. deGarassie, Nucl. Fusion 43, 142 (2003).

[35] P.C. de Vries et al. Nuclear Fusion **48**, 065006 (2008).Plasmas"

[36] Ya.I. Kolesnichenko at al., Nuclear Fusion **40**, 1326 (2000).

[37] J. Hedin et al., Nuclear Fusion 42, 527 (2002), and references therein.

[38] L.-G. Eriksson and P. Helander, Physics of Palsmas **1**, 308 (1994).

[39] P.C. deVries, et al., Plasma Phys. Control. Fusion **48**, 1693 (2006)

[40] A. Eriksson et al., Plasma Phys. Control. Fusion **49**, 1931 (2007).

[41] C. D. Challis *et al.,* Nucl. Fusion **29**, 563 (1989).

[42] T. Tala et al., Nucl. Fusion **47**, 1012 (2007).

[43] P.C. de Vries et al. Nuclear Fusion **48**, 065006 (2008).

[44] A. Ekedahl et al., Nuclear Fusion **38**, 1397 (1998).

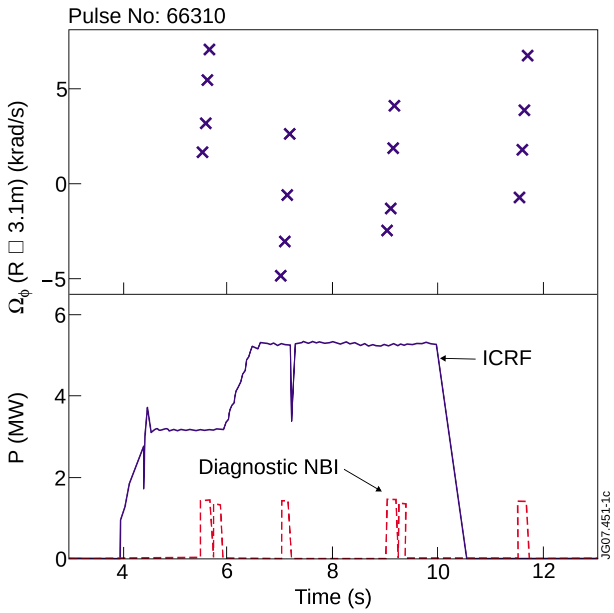

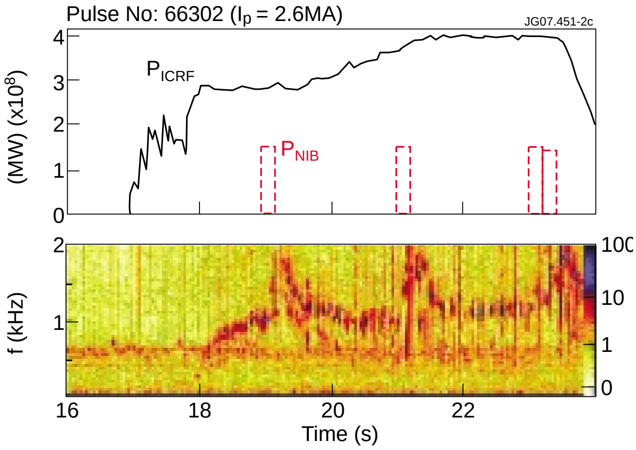

Figure 1: Typical power wave form (Pulse No: 66310, with B_T=2.6T, I_P= 1.5MA), with diagnostic NBI pulses for CXRS; and central rotation velocity deduced from consecutive CRXS spectra during an NBI pulse.

Figure 2: Power wave form (top) and spectrogram of magnetic pick up signal (bottom) for Pulse No: 66302, B_t =, I_p=. The activity found in the spectrogram is due to sawtooth precursors, and the increase their frequency indicates a co-current acceleration of the mode.

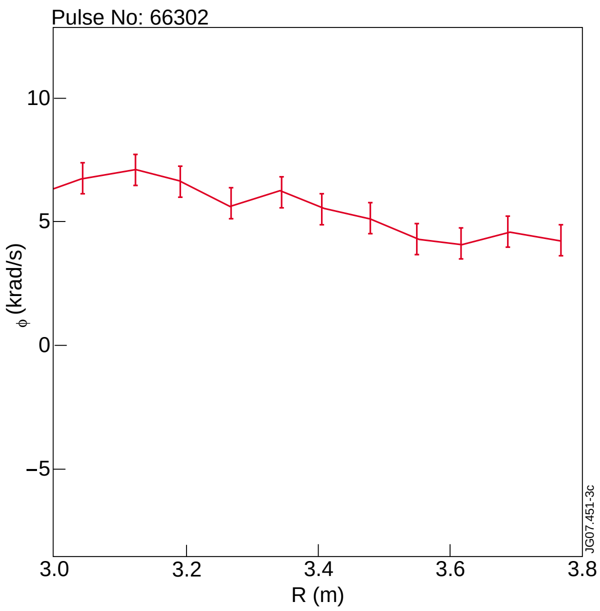

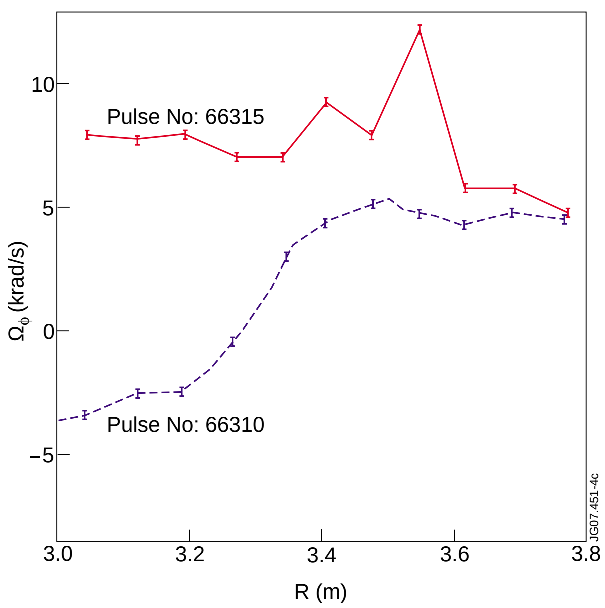

Figure 3: Rotation profile for discharge Pulse No: 66302 measured with CXRS at the beginning of the NBI pulse at t = 23.015sec (see fig.2).

Figure 4: Rotation profiles for two ICRF heated discharges taken at the third NBI pulse (t≈9s, see Fig.1): solid line, I_P = 2.6MA (Pulse No: 66315); dashed line I_p= 1.5 (Pulse No: 66310). MA.

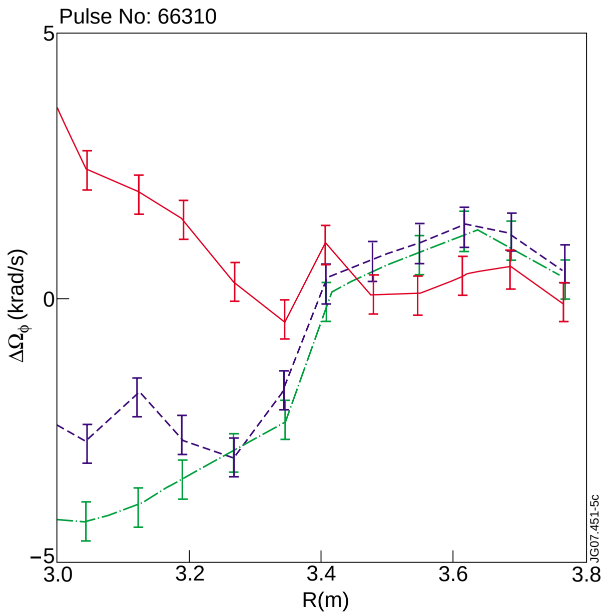

Figure 5: Change in the rotation profile compared to the Ohmic phase for Pulse No:66310. The curves were obtained by taking the difference between the rotation profiles taken at the beginning of the three first NBI pulses and the profile from the beginning of the fourth one, see Fig. 1. The solid, dot-dashed and dashed lines represent the first second and third NBI pulses respectively.

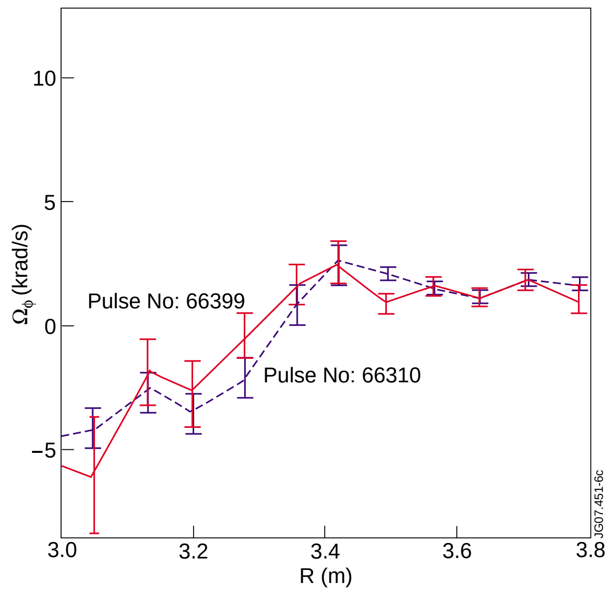

Figure 6: Rotation profiles for Ohmic Pulse No: 66399 with target parameters and NBI pulses similar to Pulse No: 66310, the plasma current was 1.6MA. The two rotation profiles are taken from the two last NBI pulses of the four that was applied, but the rotations profiles were all similar.

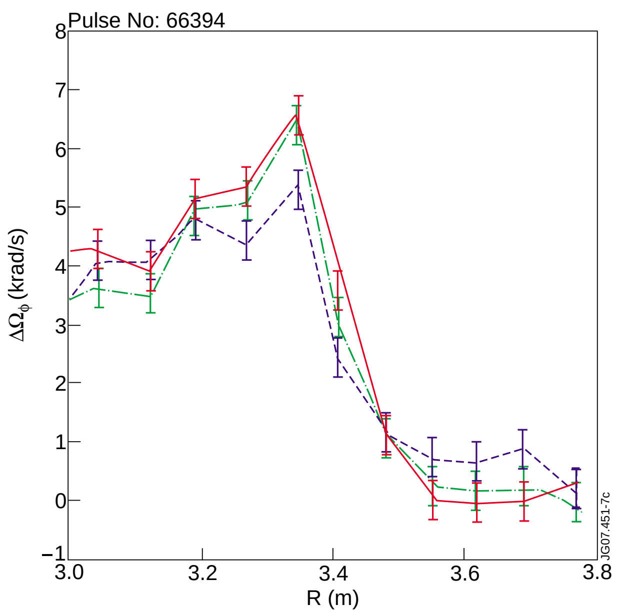

Figure 7: Change in the rotation profiles with respect the Ohmic phase for Pulse No: 66394, which had a plasma current of 2.4MA. The power wave form was similar to Pulse No: 66310 and the difference is taken for the rotation profiles from the first three NBI pulses as in Fig. 5 (red).

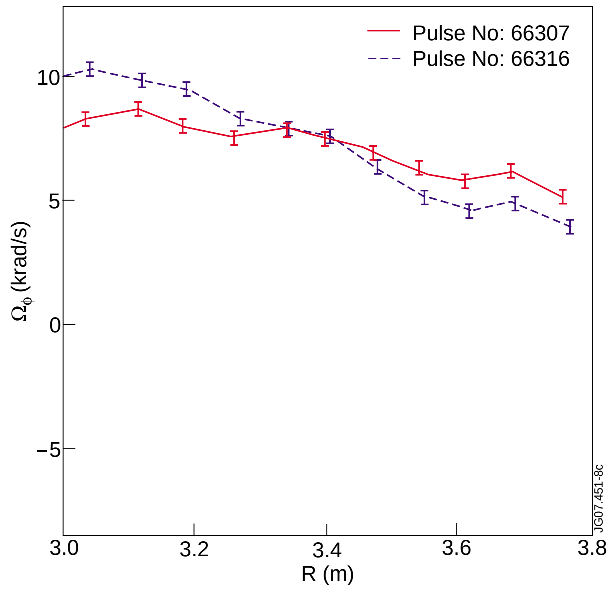

Figure 8: Rotation profiles for discharges with different hydrogen minority concentrations Pulse No: 66307 with $n_H/n_D \approx 2.5\%$ (solid line) and Pulse No: 66316 with $n_H/n_D \approx 12\%$ (dashed line)

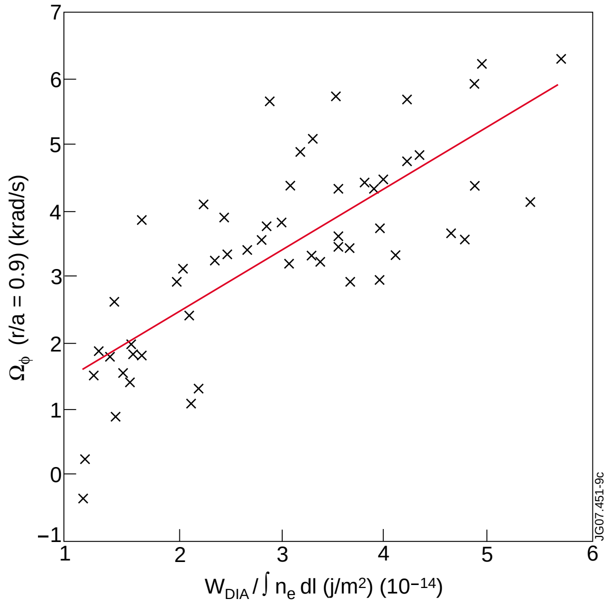

Figure 9: Edge rotation frequency, at R ≈ 3.7m, as a function the diamagnetic energy over the line integrated electron density.

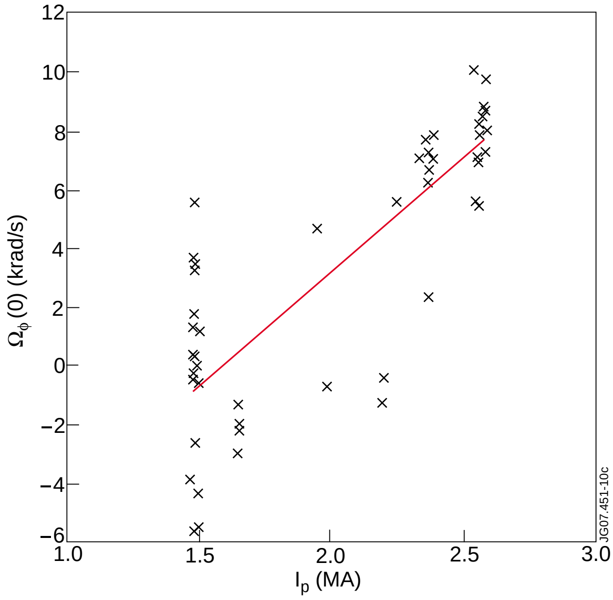

Figure 10: Central rotation frequency, at R ≈ 3.1m, as a function of the plasma current.

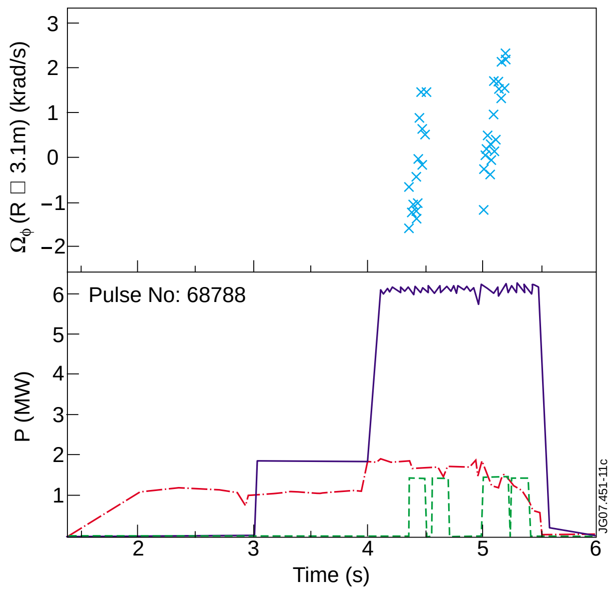

Figure 11: Power wave form for Pulse No: 68788 (bottom), solid line ICRF power, dot-dashed line LH power, dashed line diagnostic NBI; and rotation frequency near the centre at R≈ 3.1m (top figure).

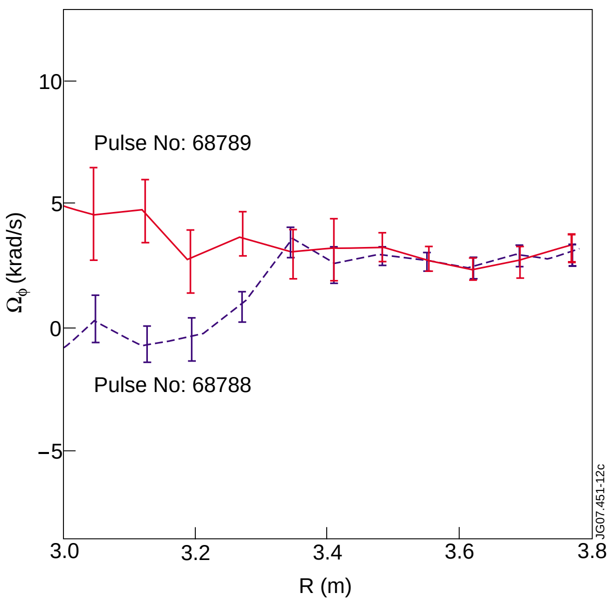

Figure 12: Rotation profiles for two discharges with LHCD; one with ICRF power Pulse No: 68788 (dashed line) and one without Pulse No: 68789 (solid line).

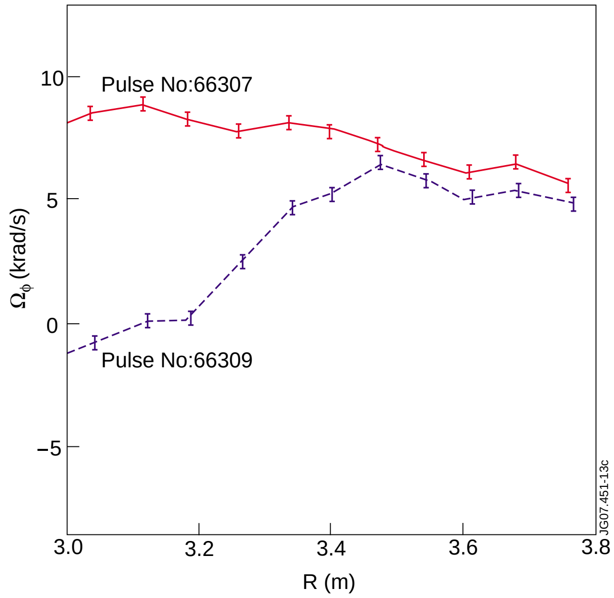

Figure 13: Measured rotation profiles taken at the third NBI pulse for Pulse No's: 66307 (solid line) and 66309 (dashed line). The former had a plasma current of 2.6MA while the latter was run with a current of 1.5MA. The influence of fast ions on the toroidal rotation for these discharges has been simulated by the SELFO code and are displayed in Fig.14.

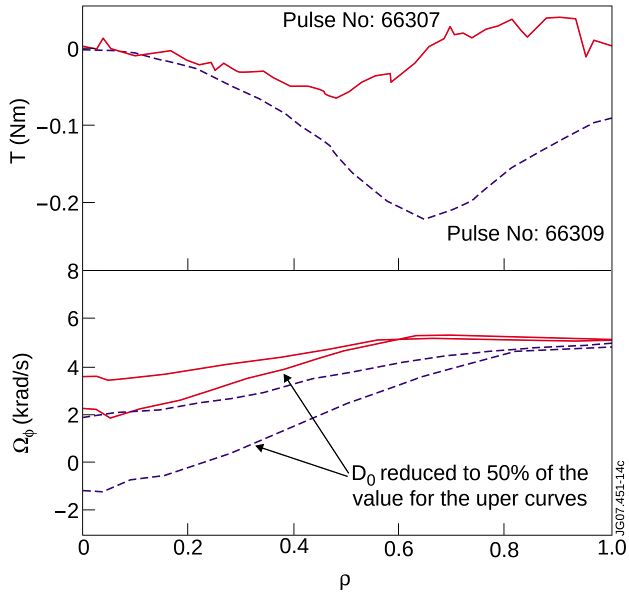

Figure 14: Top panel: volume integrated torque densities on the bulk plasma due to ICRF heated fast ions simulated by the SELFO code for the discharges in Fig.13, Pulse No's: 66307 (dashed line) and 66309 (solid line). Bottom panel: the effect of the simulated torques on rotation profiles by inserting them in a the momentum diffusion equation and taking the measured rotation frequency at R = 3.7m as a boundary condition; upper curves and lower ones.

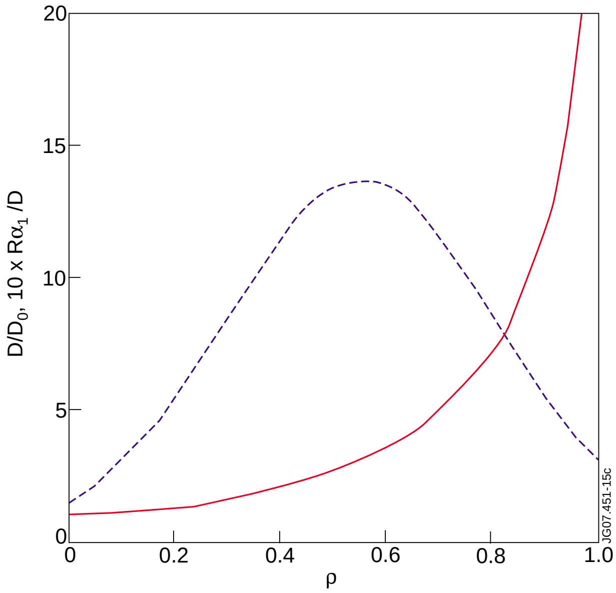

Figure 15: Coefficients in the momentum transport equation used to obtain the simulated profile of the toroidal rotation frequency shown in Fig.16.

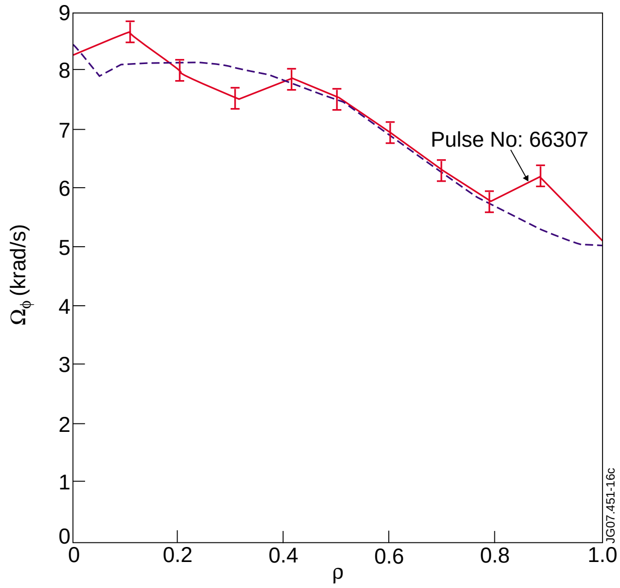

Figure 16: Mesured rotation frequency for discharge Pulse No: 66307 (solid line) and simulated profile from the torque provided by the SELFO code and the transport coefficients displayed in Fig.15 (dashed line).